Proceedings of the Korean Nuclear Society Spring Meeting
Seoul, Korea, May 1998

Environmentally Assisted Crack Growth Behavior of SA508 Cl.3 Pressure Vessel Steel

Jun Hwan Kim and In Sup Kim

Korea Advanced Institute of Science and Technology
Department of Nuclear Engineering
373-1 Kusong-dong, Yusong-gu
Taejon, Korea 305-701

Abstract

In order to assess the susceptibility of the environmentally assisted cracking(EAC) on SA508 Cl.3 steel in primary water condition, potential step test and slow strain rate test(SSRT) were conducted in a simulated crack tip condition. In this test, anodic dissolution was dominant in the crack tip environments. Proposed simple dissolution model is a modification of Hishida's anodic dissolution model at the plastic zone. One can predict actual crack growth rate with the smooth specimen through this model.

1. Introduction

Environmentally assisted cracking(EAC) is a general term for brittle material failures that result from a synergistic phenomenon between mechanical factor and a corrosive environment. It includes stress corrosion cracking(SCC), corrosion fatigue cracking(CFC), and hydrogen induced cracking(HIC). Above all, SCC and CFC have been identified as the main degradation process in nuclear power plant, as well as irradiation embrittlement

Many mechanisms and their related crack propagation models have been proposed to explain such EAC behavior. However, general ones which can cover the broad category do not exist at present. Since their behaviors are understood as a combination of the crevice corrosion and mechanical crack tip strain rate, none of them is clearly investigated. The objective of this study is to investigate the SCC behavior of SA508 Cl.3 steel and to propose its related prediction model in a moderately extensive view.

2. Experimental Procedure

2.1. Water Chemistry and Test Material

Water chemistry in this study was based on the conventional PWR primary water condition. So, experimental solution was composed of distilled water, 7500ppm H_3BO_3, and $LiOH$. To observe sulfur effect on low alloy steel, 200ppm sodium sulfate anhydrous(Na_2SO_4) was added. In order to simulate crack tip chemistry, some solutions

were de-aerated by nitrogen gas for 2 or 3 hours to expel dissolved oxygen. And pH could be controlled by step titration of *LiOH* to achieve pH of 6.98, 6.10, and 4.55. The experimental condition is shown in table 1.

Test material used in this study is ASME 508 class 3 steel. Chemical composition of the material is shown in table 2.

2.2. Test Procedure

To attain electrochemical parameter of the bare surface transient, potential step test was executed under the simulated crack tip environment. In this test, specimen is cathodically polarized for a period and the potential is then pulsed to the value of relevance with the decay current and then monitored. The facility of the test is identical to the polarization test. Slow strain rate test (SSRT) was conducted under the selected pH and potential range to get the information on the mechanical effect in the simulated crack tip region. The specimen is a round-bar type with a gage length 13mm and 3.2mm diameter. Applied strain rate is $1.923\times10^{-6}/\mathrm{sec}$. Schematic illustration of the each test facility is shown in figure 1.

3. Results and Discussion

3.1. SSRT Results

Figure 2 shows the effect of the sulfate content on SSRT curve. In this figure, slight decrease in YS, UTS was observed under simulated crack tip condition. Fractographic observation on the smooth specimen in the 200ppm lower passive region shows the typical cup and cone fracture similar to that in air. No intergranular corrosion was observed. This can be explained that anodic dissolution occurred on the entire gage length section of the smooth specimen, thus caused reduction of load bearing area.

Figure 3 shows the effect of pH on SSRT curve. The susceptibility of EAC behavior was high under the condition in which acidity and potential range were combined. It seems that acidity accelerated anodic dissolution, besides pitting mechanism. The same trend was observed in the potential step test.

3.2. Potential Step Test Results

From the potential step test, the time-decaying curve can be as follows [1];

$$i = i_0\left(\frac{t_0}{t}\right)^n$$

where i_0=bare surface dissolution current density

t_0=transient time during which bare surface current can be measured

n=repassivation exponent

The linear dependence on logi-logt behavior is caused by high-field conduction between metallic surface and solution [2]. The effect of the sulfur species and solution pH on the repassivation kinetics is shown in figure 4. The increase of the sulfur species

and the acidity delayed repassivation, caused to increase the exchange charge density and the susceptibility of the chemical attack. Combrade [3] mentioned that sulfate reduction formed monolayer, which acted on increasing dissolution current of bare surface, and delayed passive film formation, on the iron surface.

The n value with sulfate species and corrosion potential is shown in figure 5. In this figure, n value decreases with the addition of the sulfur content and degree of acidity. The decrease of n value can be represented as the reaction-controlled behavior in region II. Slight change of corrosion potential caused drastic change of n value. This is due to the large solution conductivity of the test solution [1].

3.3. Evaluation of Ford-Andresen Model

Ford derived crack propagation as the following relationship [4];

$$\frac{da}{dt} = \frac{M}{z\rho F} \frac{i_0 t_0^n}{(1-n)\varepsilon_f^n} \dot{\varepsilon}_{ct}^n$$

where ε_f=fracture strain of the film (adopted as 10^{-3})

$\dot{\varepsilon}_{ct}$=crack tip strain rate (adopted as $4.8\times10^{-13}K^4$, K : stress intensity factor)

3.4. Simple Dissolution Model

Ford-Andresen model is useful in applying LWR fields because it is based on the simple electrochemical relation as well as various experimental background. But it has some restrictions to describe a model because of difficult analysis about $\dot{\varepsilon}_{ct}$ and potential assumption in simulated crack tip. This model always starts on the assumption that passive film exists inside the crack tip. In case of high temperature condition, corrosion potential is high enough to locate above the general corrosion region of the Pourbaix diagram. But in room temperature, at which corrosion potential is relatively low, potential drop may suppress the occurrence of the passive film inside the crack [5]. Moreover, if the system in which rate-determining step in the region II is dominant either ion transport in the crack electrolyte or the environment-crack tip reaction rate exists, contribution of Ford-Andresen model will be insignificant. As it seen from SSRT result, metal will simply dissolve out as the gage length elongates in a simulated crack tip environment at room temperature.

Hishida et.al. developed a model in SSRT in relation to the simple dissolution during mechanical elongation. In plastic deformation on SSRT, he introduced a parameter, $\dot{r}_m$, which accelerates the ordinary reduction of the radius caused by the plastic strain. Using the work hardening and volume conservative equation at the plastic zone, he developed a relationship of the dimensionless parameter [6];

$$\frac{\dot{r}_m}{r_0 \dot{e}} = \frac{1}{\frac{2(\dot{e}t_m+1)^{1.5}\ln(\dot{e}t_m+1)}{n-\ln(\dot{e}t_m+1)} + \frac{2}{3}\{(\dot{e}t_m+1)^{1.5}-1\}}$$

where n=work hardening exponent

t_m=time to reach the maximum load

r_0=initial radius

$\dot{e}$=applied strain rate

Simple dissolution model proposed in this study is a semi-emperical model which is based on the similarity between plastic strain of the tensile specimen and plastic zone at the crack tip. It has an assumption that chemical reaction dominates entire process in region II. That is, if SSRT and precracked specimen are both performed in a same bulk environmental condition, differences in environment and stress state will exist between bulk and crack tip. But the changing trend in accordance with the environment will be similar. The plot of the dimensionless parameter versus actual crack growth [7,8] is shown on figure 6. From this figure, empirical relationship can be obtained with a parametric variable of E;

$$\frac{da}{dt} = A \cdot \left(\frac{\dot{r}_m}{r_0 \dot{e}}\right)^k \cdot \exp\left(-\frac{Q}{RT}\right)$$

where A, k = correlation constant

Q=activation energy (-150 kJ/mole [7])

Figure 7 is the comparison of Ford-Andresen and simple dissolution data performed in the present study. Proposed simple dissolution model can be used with or without passive/oxide film because it does not contain term related to film. Also, it is possible to predict actual crack growth with SSRT performed in the bulk environment.

4. Conclusions

From SSRT results, anodic dissolution may govern overall EAC process at the crack tip, where it is supposed to be in severe condition compared to that in bulk condition, for low alloy steel. In terms of repassivation kinetics, sulfur prevents refilming process. It increases amount of charge transfer at bare surface transient. Thus chemical reaction-dependency in region II can be predicted in Ford-Andresen model.

Proposed simple dissolution model can be used regardless of the oxide/passive film inside the crack. It shows a good agreement with the actual data.

References

[1] EPRI NP-5064M, 1987

[2] K. E. Heusler, Corr. Sci. v.39, n.7, 1997, p.1177

[3] P. Combrade, et.al., Revue de Metallurgie, Mars, 1990, p.153

[4] F. P. Ford, Corrosion, v.52, n.5, 1996, p.375

[5] B. D. Force, H. Pickering, JOM, Sep, 1995, p.22

[6] Hishida, et. al., ASTM STP 665, 1977, p.47

[7] P. M. Scott, D. R. Tice, Nucl. Eng. & Des., v.119, 1990, p.399

[8] J. Congleton, et. al., Corr. Sci., v.25, n.8/9, 1985, p.655

Table 1. Experimental conditions

	Bulk condition	Simulated crack tip condition
oxygen	aerated	de-aerated
pH	6.98	6.98, 6.10, 4.55
potential	o.c.p	active-passive(-400mV), upper passive(0mV SCE)
anion content	50ppm SO_4^{2-}	200ppm SO_4^{2-}

Table 2. Chemical composition of the test material

Chemical	Fe	C	Si	Mn	P	S	Ni	Cr	Mo	Al	Cu	V
Content(%)	Bal.	0.21	0.24	1.36	0.007	0.002	0.92	0.21	0.49	0.022	0.03	0.005

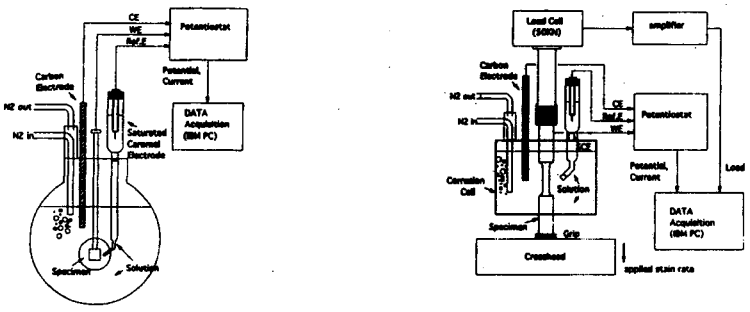

(a) (b)

Fig.1 Schematic illustration of (a) potential step test (b) SSRT

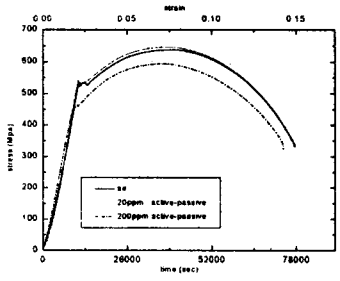

Fig.2 Effect on sulfate content of SSRT

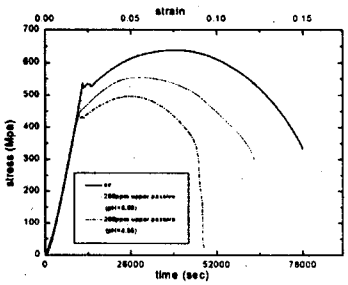

Fig.3 Effect on acidity and potential of SSRT

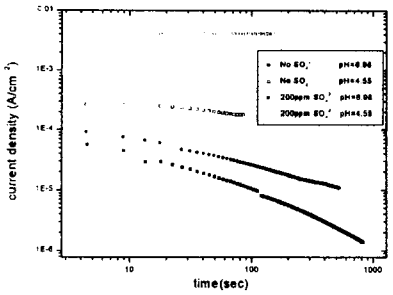

Fig.4 Delayed repassivation with acidity and sulfate content in potential step test

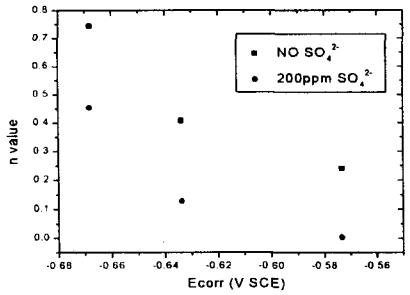

Fig.5 n value with environmental variables

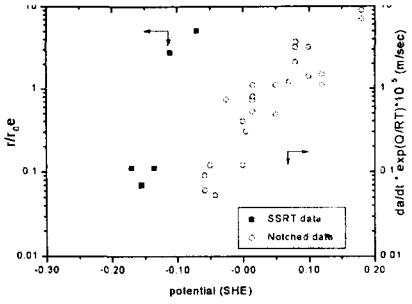

Fig.6 Dimensionless parameter and actual crack growth

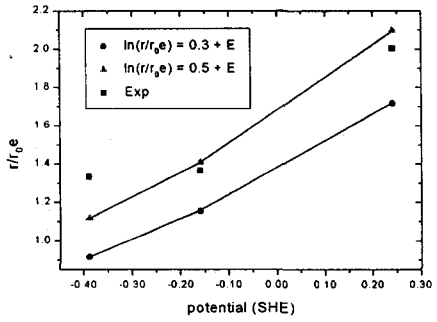

Fig.7 Comparison with extrapolated data and actual data

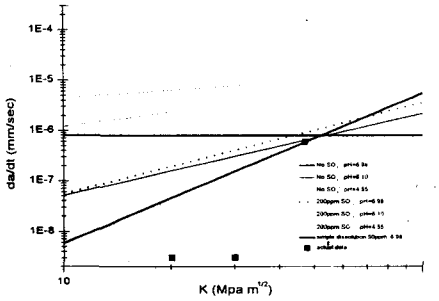

Fig.8 Comparison of each model

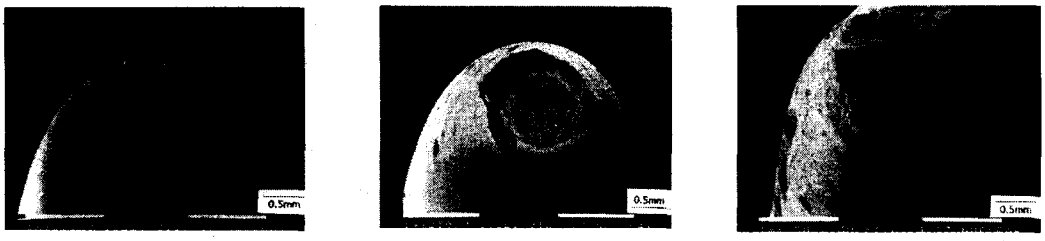

(a) (b) (c)

Fig.9 Fractographic observation on smooth specimen
(a)air, (b)200ppm SO_4^{2-}, lower passive (c)200ppm SO_4^{2-}, upper passive, pH=4.55